Mon. Not. R. astr. Soc. (1977) **178**, 473–487

A0035 'the cartwheel' a large southern ring galaxy

R. A. E. Fosbury *Anglo-Australian Observatory, PO Box 296, Epping, New South Wales 2121, Australia*

T. G. Hawarden *UK Schmidt Telescope Unit of the Royal Observatory Edinburgh, Private Bag, Siding Spring Observatory, Coonabarabran, New South Wales 2857, Australia*

Received 1976 May 24

Summary. Spectrophotometric scans and direct photographs have been obtained of the ring galaxy A0035. The Hubble distance of the system is 150 Mpc and the diameter of the ring 54 kpc. The observed radial velocities are interpreted in terms of a model where a companion galaxy has free-fallen through the centre of a massive spiral or S0 galaxy along a path which is very closely normal to the plane of the disk. The companion galaxy is identified and shown to be at a distance from the disk which corresponds to a time of 3×10^8 yr since the closest approach. This figure agrees with the expansion timescale of the ring deduced from the measured expansion velocity and the present radius. From the rotation velocity of the ring, the mass of the nucleus of the galaxy is shown to be in the region of $4 \times 10^{11} M_\odot$. The ring consists of giant photoionized H II regions with individual absolute magnitudes in the range $-18 \lesssim M_B \lesssim -17$. The total mass of ionized gas in the ring is $\gtrsim 1.2 \times 10^8 M_\odot$. No evidence for ionized gas is found either within the area outlined by the ring or in the companion galaxy. The integrated H_β luminosity of the H II regions implies the presence of about 3×10^5 O-stars providing Lyman continuum photons, but the energy distribution of the optical continuum implies that the number of O- and B-stars must be closer to 3×10^6. The expected frequency of Type II supernovae in the system could therefore be as high as one per year. Elemental abundances have been measured for two of the H II regions. Oxygen, nitrogen and neon are deficient by factors of 6 ± 2, 22 ± 4 and 3 ± 2 respectively when compared with the Orion Nebula in our Galaxy. These low abundances imply either that the whole system is young or that the gas that has been swept out of the original disk by the expansion of the ring has been mixed with a massive halo of primordial gas. We prefer the latter interpretation and identify this halo with the H I annuli which are now being found by 21-cm observations of S0 and later-type galaxies. A 21-cm observation of the A0035 system gives an upper limit on the mass of neutral hydrogen of about $10^{11} M_\odot$.

1 Introduction

As a member of the rare class of ring galaxies A0035 has a spectacular appearance with a bright, sharp outer ring attached tu an inner ringed nucleus by spiral 'spokes'. Amongst those with measured Hubble distances, its outer ring has the largest linear diameter.

The galaxy was discovered originally by Zwicky (1941), catalogued by de Vaucouleurs & de Vaucouleurs (1964), reported by Lü (1971), and catalogued by Vorontsov-Vel'yaminov & Arkhipova (1974) under the designation MCG 6-2-22a. It was rediscovered by R. D. Cannon during inspection of the IIIaJ *Sky Survey* plates taken with the UK 48-in Schmidt telescope in Australia and appears in the Royal Observatory Edinburgh preliminary catalogue of southern peculiar galaxies (Arp & Madore 1975).

Only about a dozen such objects have been reported in the literature (Cannon, Lloyd & Penston 1970; Freeman & de Vaucouleurs 1974; Graham 1974; Lynds & Toomre 1976 and references therein), but several more have recently been discovered during inspection of the southern Schmidt sky surveys both in Australia and Chile (Hawarden, Graham, private communication).

Freeman & de Vaucouleurs (1974) proposed an explanation of the morphology of two supposedly related classes of ring galaxy in terms of a collision between a gas-rich spiral and an intergalactic gas cloud which was probably originally neutral. According to them the collision results in the separation of the annular gas content of the spiral and its spheroidal, predominantly stellar, nucleus. If the motion was normal to the disk of the spiral, the collision resulted in a gaseous ring, while in less favourable geometries the remaining gas was chaotic and multinucleated.

In a number of objects, A0035 being a particularly fine example, the ring clearly contains its own nucleus as well as having a nearby spheroidal companion which is presumably associated. It was Theys (1973) who noticed that the companion galaxy frequently lay along the projection of the minor axis of the ring. Since then Lynds & Toomre (1976) have presented model calculations to explain the morphology of the remarkable double ring galaxy II Hz 4.

In this paper we present detailed observations of the A0035 system and show how these are consistent with the interaction picture of Lynds & Toomre. We also suggest that observations of ring galaxies are important in the study of the gas contents of spiral and S0 galaxies.

2 Observations

Three plates have been taken of the field containing A0035 with the UK 48-in Schmidt telescope. Two (J739 (1974) and J1621 (1975)) were taken on N_2 sensitized IIIaJ behind a GG395 filter, and the other (R1923 (1975)) on 098-04 emulsion with an RG630 filter. The red plate does not reach such a faint limiting magnitude but does allow a better estimate to be made of the relative surface brightness of some parts of the ring and the nearby galaxies. The reproductions in Plates 1 and 2 are from J1621 the latter being taken from a high contrast positive copy.

Spectrophotometric scans of a number of regions around the ring and in the nucleus and of the two nearby galaxies have been made with the image-dissector scanner (Robinson & Wampler 1972, 1973) on the 3.9-m Anglo-Australian Telescope (AAT). The regions that have been observed are identified on Plate 1 and the individual observations, together with the relevant parameters, are listed in Table 1.

Two different spectrographs and scanner modules were used for these observations and are identified as systems I and II in Table 1. System I consisted of a spectrograph on loan

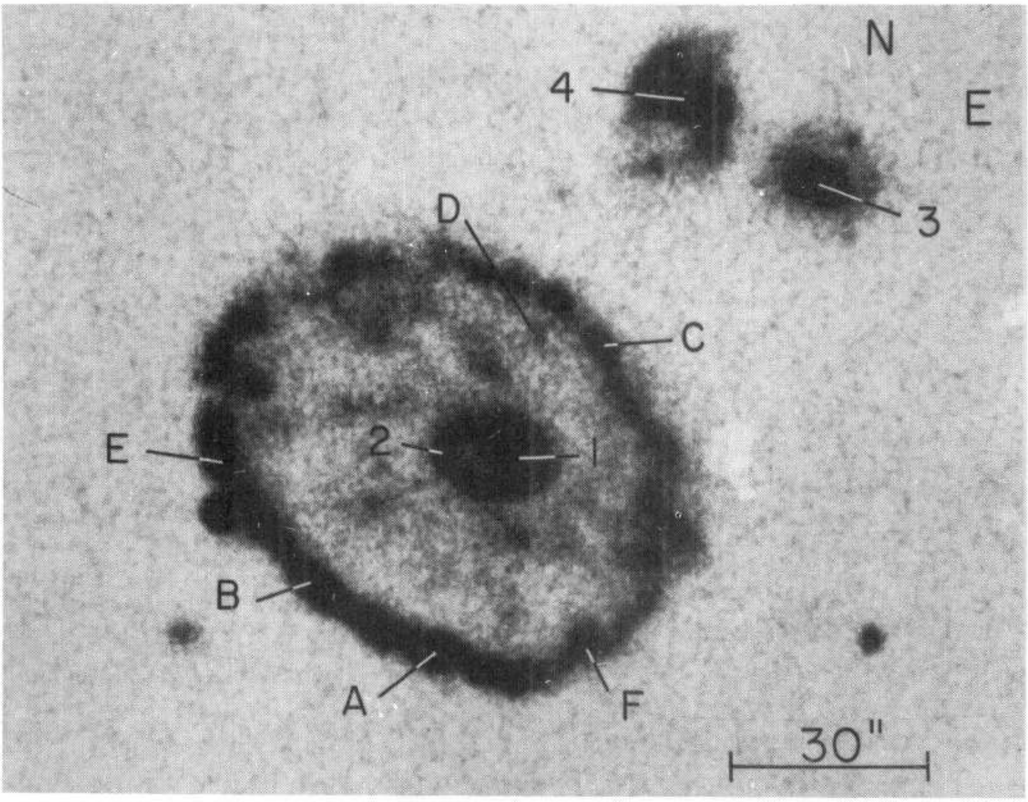

Plate 1. A0035 and companion galaxies reproduced from a IIIaJ plate taken with the UK 48-in Schmidt telescope.

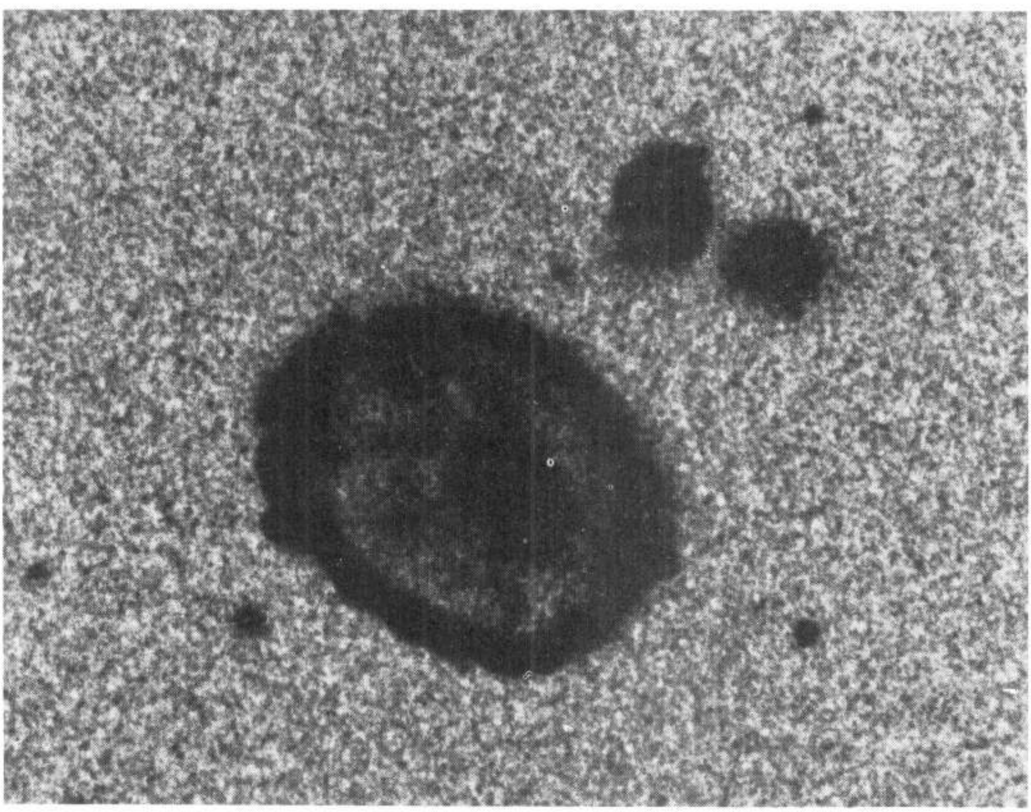

Plate 2. A high contrast copy of the same IIIaJ plate as Plate 1 showing the rather sharp outer boundary of the ring.

Table 1. Log of scanner observations and observed radial velocities.

Date	Region	Wavelength coverage (Å)	Integration (min)	Spectrograph system	Heliocentric velocity ($km\,s^{-1}$)	Internal sd
1975 August 8/9	1	3300–5860	96	I	9212	180
1975 August 8/9	A	3300–5860	72	I	9281	57
1975 August 8/9	3	3300–5860	16	I	9104	130
1975 August 8/9	C	3300–5860	48	I	9071	57
1975 August 8/9	4	3300–5860	16	I	8639	33
1975 August 8/9	2	3300–5860	8	I	–	–
1975 August 8/9	B	3300–5860	16	I	9110	66
1975 August 8/9	D	3300–5860	8	I	–	–
1975 November 2/3	A	5590–7640	44	II	9246	12
1975 November 25/26	E	3860–5900	20	II	9045	36
1975 November 25/26	F	3860–5900	4	II	9264	27
1975 November 25/26	A	3860–5900	4	II	9234	40

from the Lick Observatory. This had a 600-line mm^{-1} grating and worked at the $f/8$ Cassegrain focus of the AAT. The star and sky apertures each measured 3 × 6 arcsec and were separated by 34 arcsec in RA. The resulting spectral resolution was 10 Å (FWHM). The first image-tube in the scanner chain had an ultraviolet-transmitting fibre-optic faceplate, allowing observations to be made down to the atmospheric cut-off. System II consisted of the fast Cassegrain spectrograph at the $f/15$ focus of the AAT. The star and sky apertures in this case were 2 × 4.5 arcsec and separated by 20 arcsec in RA. A 1200-line mm^{-1} grating was used, giving a spectral resolution of 4 Å. In this system the faceplate of the first image-tube limited the available wavelength range to longward of about 3800 Å.

Photometric standard stars – from Oke (1974) – were observed with the same system on the same nights in order to calibrate the spectral response. Methods of sky subtraction, reduction and wavelength calibration have been described elsewhere (Robinson & Wampler 1972). Scans of regions A, B, C, 1, 3 and 4 are reproduced in Figs 1, 2 and 3.

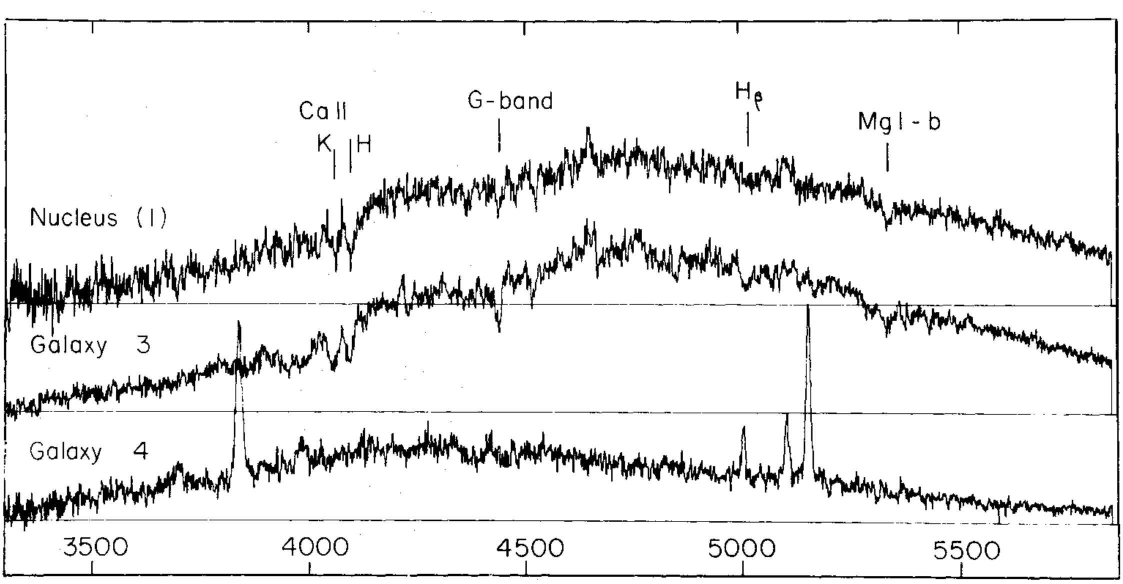

Figure 1. Scans of the nucleus of A0035 and the two companion galaxies. These are plotted on the observed wavelength scale.

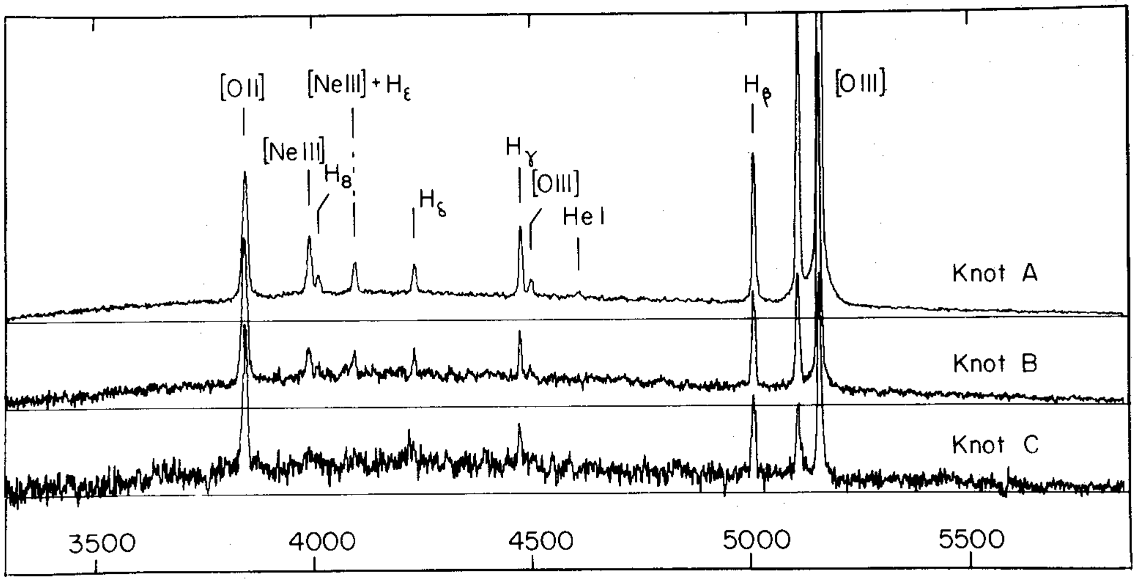

Figure 2. Scans of three of the H II regions in the ring.

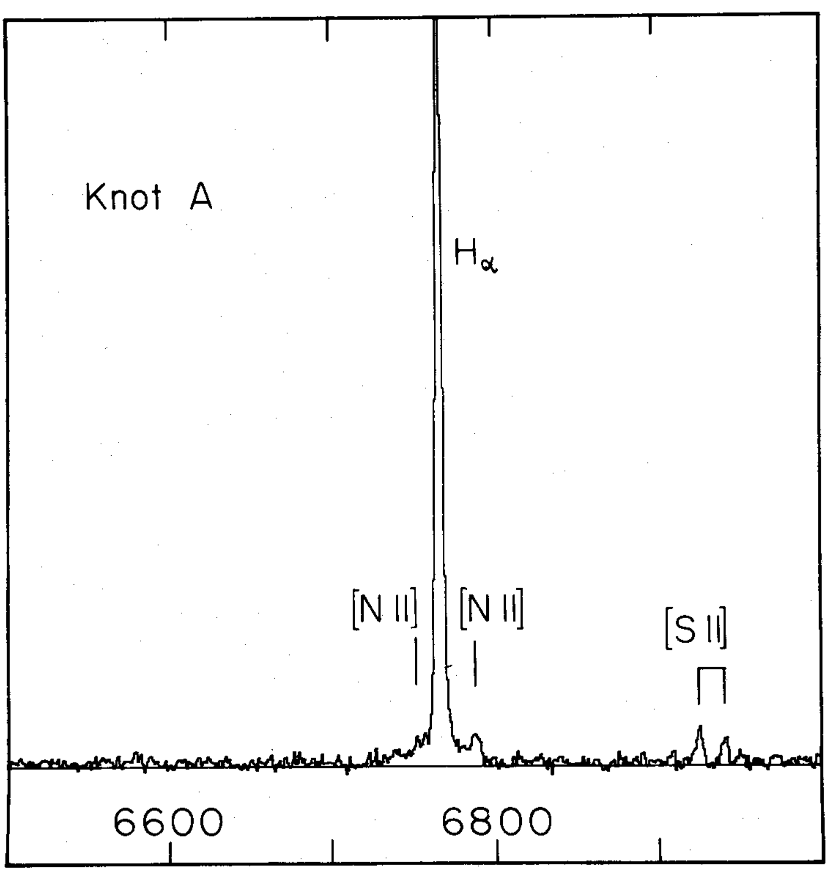

Figure 3. Part of the red scan of the brightest H II region.

Plate 3 shows two frames taken from the slit-viewing television system of the AAT during the scanner observations with system I. The seeing was $\lesssim 1$ arcsec and the pictures illustrate the sharpness of the ring and also, incidentally, the advantages of this type of slit-viewing system for knowing exactly what is going down the scanner aperture.

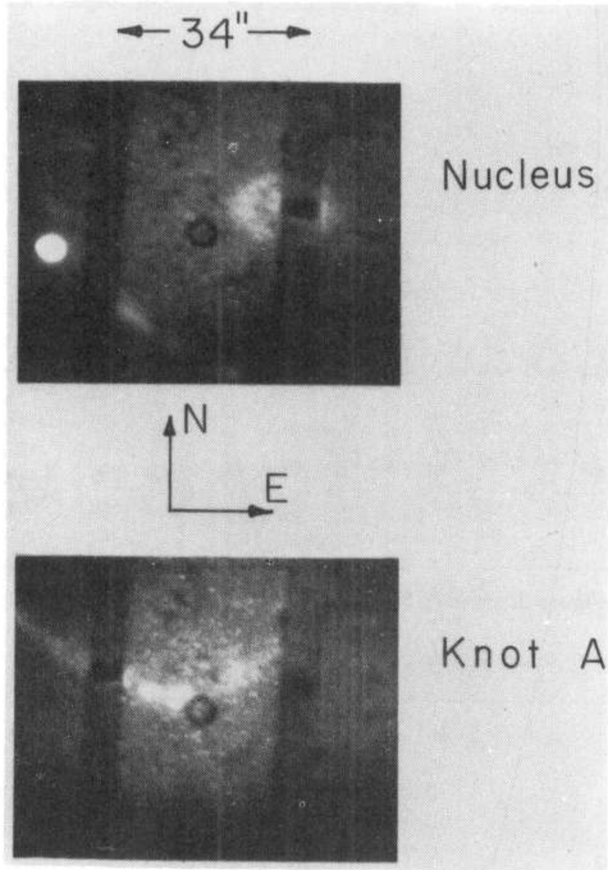

Plate 3. The appearance of A0035 on the slit-viewing TV system of the AAT. Note the sharpness of the ring (the apertures are 3 × 6 arcsec) and the inner ring surrounding the nucleus.

Using the Parkes 64-m telescope, the position of A0035 has been searched for 21-cm H I line emission around a frequency band corresponding to the optical systemic velocity of the system. No emission was detected but, making some assumptions about the expected line width by reference to the optical observations, an upper limit of $\sim 10^{11} M_\odot$ has been placed on the mass of neutral hydrogen present.

3 Analysis

All of the knots observed around the outer ring (A, B, C, E and F) have emission lines and a blue continuum which show them to be relatively normal, though as we shall show later, exceedingly luminous H II regions photoionized by hot stars. No emission lines have been detected inside the ring, i.e. in regions 1, 2 and D, and in particular the nucleus shows a late-type stellar absorption spectrum with the Ca II H and K lines, the G-band and the Mg I b-band being readily detected. Of the two nearby galaxies, 4 has a blue continuum with emission lines while 3 is interesting in that it shows no evidence of containing any ionized gas and has an unusually high surface brightness.

The radial velocities of regions A, B, C, E, F, 1, 3 and 4 have been determined from the scanner observations. When measuring the emission lines, the internal scatter has a standard deviation of about 40 km s^{-1} when measurements are made with both systems I and II. The relative velocities, however, should have an error significantly less than this. For those regions which only show absorption lines, the internal standard deviation is approximately 150 km s^{-1}. The heliocentric velocities, together with their respective internal standard deviations, appear in Table 1.

3.1 DYNAMICS

In order to study the dynamics of the system, it is first of all assumed that the ring is circular (see Lynds & Toomre 1976). The measured values for the lengths of the major and minor axes of the approximately elliptical distribution of bright knots are then used to derive the angle of inclination. If i is defined to be the angle between the normal to the ring and the line of sight, then

$$\cos i = \frac{\text{minor axis}}{\text{major axis}} \quad \text{and} \quad i = 40^\circ \pm 1.$$

It is now possible to describe the position of each of the observed knots around the ring by the angle θ between the line joining the knot to the centre of the deprojected ring and the south-eastern extension of the observed major axis. θ increases as we move from the north-east to the north-west quadrant. If it is assumed that all the internal motions are in the plane of the ring, then the observed radial velocity of a particular knot can be represented by an expression of the form

$$V(\theta) = V_{\mathrm{SYST}} + \sin i (V_{\mathrm{t}} \cos \theta + V_{\mathrm{r}} \sin \theta)$$

where V_{t} and V_{r} are the velocities in the tangential and radial directions respectively. Fig. 4 shows the observed heliocentric velocities of knots A, B, C, E and F plotted against the angle θ. The continuous line is a least-squares fit of the function defined above to these five points. The fit gives $V_{\mathrm{SYST}} = 9100$, $|V_{\mathrm{t}}| = 254$ and $|V_{\mathrm{r}}| = 89\ \mathrm{km\ s^{-1}}$. If the additional assumption is made that the spiral 'spokes' trail, then V_{r} represents a radial *expansion* and the north-east is the side of the ring nearest us. Treating the expansion as a small perturbation, the mass of the nucleus can be estimated from the tangential velocity of the ring using the usual circular approximation. Taking the Hubble constant $H_0 = 60\ \mathrm{km\ s^{-1}\ Mpc^{-1}}$, the observed systemic velocity and the angular semi-major axis of 37 arcsec give a linear radius R of 27 kpc and a

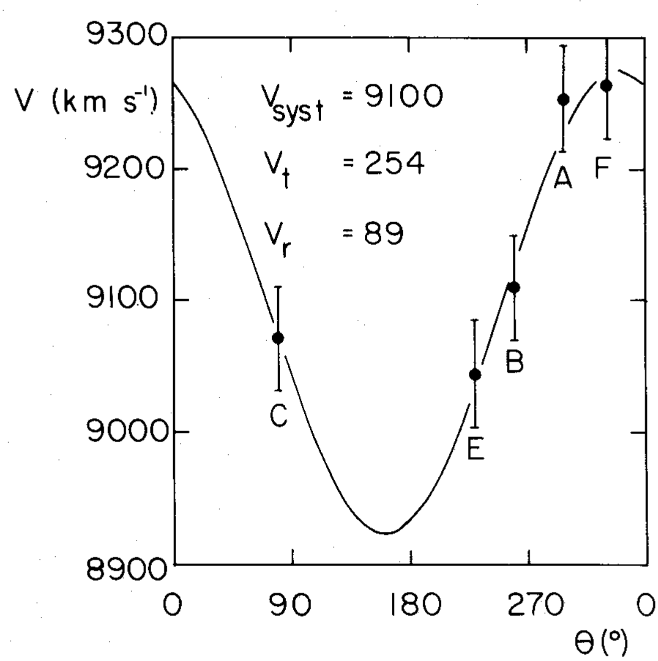

Figure 4. The heliocentric velocities of five of the H II regions plotted against the position around the ring. The solid line is a least-squares fit of a sinusoidal function yielding the indicated fit parameters (in $\mathrm{km\ s^{-1}}$).

distance of 152 Mpc. The nuclear mass M_n is then given by

$$M_n \simeq \frac{V_t^2 R}{G} = 4 \times 10^{11} M_\odot .$$

It is immediately clear that we are dealing with a very large and massive system. Indeed, amongst the relatively small number of ring galaxies which have measured systemic velocities (Freeman & de Vaucouleurs 1974; Graham 1974; Lynds & Toomre 1976), A0035 has the largest linear diameter.

A direct estimate can be made of the age of the ring by identifying it with the expansion timescale

$$t_e = \frac{R}{V_r} \simeq 3 \times 10^8 \text{ yr}.$$

This value will later be compared with another, more model-dependent, age estimate.

The radial velocities of the nucleus (region 1) and galaxy 3 are both within one standard deviation of the systemic velocity of the ring. Galaxy 4, however, has a velocity which is lower by some 400 km s^{-1}. On the strength of these velocities and the fact that galaxy 3 does not show evidence of containing ionized gas it is argued that, of the two companions, galaxy 3 is the more likely to be associated with the ring phenomenon.

3.2 LUMINOSITIES

The scanner observations are calibrated with respect to standard stars and thus give a direct measure of the apparent brightness of the various components of the A0035 system. These measures are limited in accuracy due to the fact that the scanner apertures are small by photometric standards, but it is believed that the *B*-magnitudes and H_β fluxes we derive have systematic errors which are smaller than half a magnitude. Only those observations made with system I are used to derive this photometric information, mainly because this had the largest apertures, though there are other instrumental reasons for believing that these have the greatest accuracy. The results appear in Table 2.

The H_β fluxes are derived from the H_β equivalent widths (Table 3) and the observed *B*-magnitudes. Neither the absolute magnitudes nor the H_β luminosities have been corrected for extinction: a value of $E_{B-V} = 0^m.64$ is later derived for knots A and B from the Balmer decrement, but the reddening is likely to be predominantly internal. This problem is considered again when we discuss the optical continuum of the H II regions.

Given the H_β luminosities of the knots A, B and C, an estimate can be made of the total H_β luminosity of the ring and thence, given an estimate of the mean electron density, the total mass of ionized gas in the system. From Plate 1 we can count ten knots with an apparent

Table 2. Magnitudes and H_β – fluxes.

Region	m_B	M_B	$F(H_\beta)$ (erg cm^{-2} s^{-1})	$L(H_\beta)$ (erg s^{-1})
A	17.8	−18.1	4.4×10^{-14}	1.2×10^{41}
B	18.1	−17.8	2.2×10^{-14}	5.7×10^{40}
C	18,2	−17.7	1.6×10^{-14}	4.2×10^{40}
1	18.8	−17.1	–	–
3	17.1	−18.8	–	–
4	18.3	−17.6	–	–

brightness about equal to knot B and another ten about equal to knot C. If it is assumed that the H_β equivalent widths are similar in all these knots (the scans of E and F give us confidence in this assumption), then the total H_β luminosity of the ring is

$$L(H_\beta)_{ring} \simeq 1 \times 10^{42}\ \mathrm{erg\ s^{-1}}.$$

A mean electron density in knot A can be measured from the observed intensity ratio of the [S II] doublet λλ 6716, 6730 (Fig. 3). Using the atomic data given in Saraph & Seaton (1970) we find that $N_e \lesssim 10^2\ \mathrm{cm^{-3}}$. Taking this upper bound to apply also to the other knots, we can derive the total proton number

$$N_p V = \frac{L(H_\beta)}{h\nu_{H_\beta}\alpha^{eff}_{H_\beta} N_e}$$

$$\gtrsim 1.1 \times 10^{65}\ \text{protons}$$

where we have used $\alpha^{eff}_{H_\beta}$ ($T_e = 15\,000$ K) interpolated from the values given in Osterbrock (1974). The total mass of the H II regions is then

$$M_{H\,II} = \mu m_H N_p V$$

$$\gtrsim 1.2 \times 10^8\ M_\odot$$

where μ, the mean mass per proton, is taken to be equal to 1.4.

3.3 ELEMENT ABUNDANCES

The spectrum of knot A was observed for sufficiently long to obtain a rather high signal-to-noise ratio with a view to obtaining accurate relative emission line intensities and hence physical conditions and element abundances. Even a cursory comparison with the spectrum of Galactic H II regions like M42 in Orion shows that the gas in the A0035 ring has a significantly higher electron temperature than is usual in photoionized gas with normal abundances (note the great strength of the λ 4363 [O III] line in Fig. 2). Since the spectra are otherwise similar to ordinary H II regions, i.e. no evidence for shock heated gas which would be provided by strong [S II] and [O I] lines, the high electron temperature can be interpreted in terms of a low oxygen abundance resulting in a reduced cooling efficiency. Knot A is not unique in this respect since the spectrum of knot B, though of lower signal-to-noise, also shows the strong λ 4363 line. These statements can be made quantitative by deriving the emission line intensities in knots A and B and, after correcting for interstellar reddening, subjecting these to the usual type of abundance analysis.

The equivalent widths and intensities relative to H_β of the emission lines in knots A and B are given in Table 3. The conversion to relative intensity is made by using the scans of standard stars made with the same system on the same night. A reddening corresponding to $E_{B-V} = 0.64$ is derived by comparing the observed Balmer line intensities with those predicted by case B radiative recombination theory (Osterbrock 1974) and assuming a normal interstellar reddening law. The last columns of Table 3 give the relative line intensities corrected for this reddening. The intensities of [N II] λ 6583 and [S II] λλ 6716, 6730 have been expressed relative to H_β directly by assuming a radiative $I(H_\alpha)/I(H_\beta)$ ratio. The individual intensities for [Ne III] λ 3967 and H_ϵ have been derived from the blended feature by using the known [Ne III] branching ratio.

Table 3. Emission line equivalent width and intensities in knots A and B.

Line		Equivalent width (Å) A	B	I ($H_\beta \equiv 100$) A	B	I ($H_\beta \equiv 100$) corr A	B
3727	[O II]	95.8	102.2	183	353	382	736
3835	H_9	2.3	–	3.9	–	7.5	–
3868	[Ne III]	26.6	13.6	42	41	79	77
3888	H_8 + He I	9.2	4.2	14.2	12.2	27	23
3967	[Ne III] }	13.6	9.2	22	26	26	26
3970	H_ϵ }					13	20
4101	H_δ	11.8	6.6	16.0	16.8	26	27
4340	H_γ	33.7	12.6	36	27	48	36
4363	[O III]	8.5	3.4	9.1	7.3	12.2	9.8
4471	He I	3.0	–	3.0	–	3.7	–
4861	H_β	112.8	61.9	100	100	100	100
4958	[O III]	278	98	217	152	207	145
5006	[O III]	869	314	714	466	667	435
6562	H_α	–	–	–	–	280	–
6583	[N II]	–	–	–	–	8.4	–
6716	[S II]	–	–	–	–	11.5	–
6731	[S II]	–	–	–	–	7.9	–

The electron temperature is determined from the [O III] line ratio using the collision strengths given by Seaton (1975). These give

$$\frac{I(\lambda 4958) + I(\lambda 5006)}{I(\lambda 4363)} = 7.2 \exp\left(\frac{32970}{T_e}\right)\left[\frac{1 + 0.00054x}{1 + 0.063x}\right]$$

where

$$x = \frac{10^{-2} N_e}{T_e^{1/2}}$$

Assuming the [S II] density limit holds for knot B also, collisional de-excitation is negligible and we find that

T_e (knot A) = 14 300 ± 1000 K

and

T_e (knot B) = 18 000 ± 2000 K

the quoted error representing an uncertainty in the measured value of $I(\lambda\, 4363)$.

In what follows we shall make the simplest possible assumptions, i.e. that the gas has uniform kinetic temperature and electron density and also that hydrogen is fully ionized in the regions where the forbidden lines are formed (so $N_p = N_H$). Then the abundance ratio of the ion in question relative to hydrogen is given by

$$\frac{N_i}{N_H} = 23.8 \frac{I(\lambda)}{I(H_\beta)} \frac{\alpha_{H_\beta}^{eff}(T)\, \lambda T^{1/2} \exp(h\nu/kT)}{\left(\frac{\Omega(1,2)}{\omega_1}\right) b}$$

where $\Omega(1, 2)$ is the collision strength of the forbidden line and ω_1 the statistical weight of the lower level. b is the fraction of excitations to level 2 which result in the emission of a photon in the line observed. ν and λ refer to the forbidden line and λ is measured in Ångström

Table 4. Ionic abundances relative to hydrogen.

	He^+	O^+	O^{++}	N^+	Ne^{++}
knot A	8.0×10^{-2}	4.1×10^{-5}	8.4×10^{-5}	6.9×10^{-7}	3.1×10^{-5}
knot B	–	5.0×10^{-5}	4.0×10^{-5}	–	1.9×10^{-5}

Table 5. Element abundances (logarithmic with H = 12.00)

	He	N	O	Ne
A0035 A	10.86	6.33	8.10	7.66
A0035 B	–	–	7.96	7.64
Orion (PTP)*	11.00	7.67	8.89	8.16
⟨LMC⟩ (PTP)	10.92	7.10	8.58	7.94
⟨SMC⟩ (Dufour)	10.97	6.49	8.05	7.18

* PTP, Peimbert & Torres-Peimbert (1974); Dufour, Dufour (1975).

units. The collision strengths for [O III], [N II] and [Ne III] are taken from Seaton (1975) while that for [O II] and the effective recombination coefficient (interpolated to the appropriate T) are from the compilation by Osterbrock (1974).

Using the line intensities given in the last column of Table 3, we derive the ionic abundance ratios given in Table 4. Assuming now that the first and second ionization stages dominate and that the nitrogen and neon ionization ratios are similar to that of oxygen, the abundances given in Table 5 are derived. The value for helium comes from a measurement of the λ 4471 line in knot A and therefore can only really be taken as an indication that the helium abundance is not grossly abnormal. It is assumed that all the helium is singly ionized and the value of $\alpha^{\text{eff}}_{\lambda 4471}$ is again taken from Osterbrock (1974) interpolated to the appropriate temperature, giving

$$\frac{N_{\text{He}}}{N_{\text{H}}} = 2.09 \frac{I(\lambda 4471)}{I(\text{H}_\beta)}$$

Apart from the question of the validity of the simplifying assumptions, the major source of uncertainty is the measurement of the intensity of the [O II] doublet λ 3727, since this depends quite strongly on the assumed reddening. The value of $I(\lambda 3727)$ affects the nitrogen and neon abundances through the value of the first to second ionization ratio we assume. If the reddening has been overestimated, the value of $I(\lambda 3727)$ is too large and the oxygen and neon abundances will come out too high, and the nitrogen too low. To illustrate the magnitude of this effect, the abundances which result from assuming that $E_{B-V} = 0.30$ instead of 0.64 are as follows:

oxygen: 7.97; nitrogen: 6.46; neon: 7.43.

4 Discussion

The foregoing analysis has provided a set of quantitative data which will allow us to discuss in some detail the origin and evolution of this ring system. The conclusions we reach should be relevant, not only to the general problem of the ring galaxies, but also to that of the nature of the gaseous content of disk-like galaxies, be they spirals, S0's or lenticulars.

Lynds & Toomre (1976) have presented model calculations which show rather convincingly that a sharp, well-defined ring structure can be produced by a particular type of galaxy–galaxy encounter. The example they consider is the remarkable double ring system II Hz 4, but their spectroscopy failed to detect any significant velocity structure. Apart from determining the distance and size of the system and placing an upper limit on its mass, they were therefore restricted to a morphological comparison. In their model, a transient ring develops as the result of a companion galaxy dropping right through a target disk galaxy on a trajectory which is almost normal to the disk and passing very close to its centre. This type of interaction would of course be expected to occur only rarely, and Lynds & Toomre justify their model by arguing that the ring galaxies do indeed have a very low space density. Theys (1973) apparently noticed the frequent presence of companions near the apparent minor axes of the known ring galaxies: A0035 is no exception, having in fact two companions very close to the projected minor axis.

Galaxy 4 (Plate 1) we believe not to be closely associated with the ring system for the following reasons. The large velocity with respect to the systemic velocity of the ring and the presence of ionized gas in galaxy 4 have been mentioned above. Also it has a rather normal, undisturbed spiral structure. If galaxy 3 ever did contain any ionized gas, it could have been swept out by a passage through the disk of a more massive spiral. If 3 is indeed accepted as the interacting galaxy then, by measuring its present distance from the centre of the ring, we can estimate the time elapsed since closest approach. To make this estimate it will be assumed that the nucleus of the ring and galaxy 3 behave like point masses and that 3 free-falls through the nucleus exactly along a normal to the disk. Also we assume that the mass of the ring nucleus is significantly greater than the mass of galaxy 3 (though this is really perhaps only by a factor of 2 or 3). The free-fall time $T_{\rm ff}$ for galaxy 3 to move from a distance R to the centre of the ring, assuming it started from infinity, is then given by

$$T_{\rm ff} \simeq \int_0^R \frac{r^{1/2}}{(2GM_{\rm n})^{1/2}}\,dr = \frac{\sqrt{2}R^{3/2}}{3(GM_{\rm n})^{1/2}}$$

Now the deprojected distance from the centre of the ring to galaxy 3 is 53 cosec 41° = 80 kpc and the time since closest approach consequently 2.5×10^8 yr. The agreement of this figure with the ring expansion timescale (3×10^8 yr) gives us confidence in the identification of 3 as the interacting galaxy and indeed with the validity of the Lynds & Toomre scheme for modelling the A0035 system. The expected difference between the systemic velocity of the ring and that of galaxy 3 is, on this simple model, 150 km s^{-1}. The observed velocity difference is close to zero but the observational uncertainty is of the same order as the expected difference. The observed displacement of the nucleus from the geometric centre of the ring can be explained as a combination of two effects. Firstly, during the interaction the nucleus tries to follow the intruder and consequently becomes non-coplanar with the ring, i.e. a projection effect. Secondly, a result of the intruder not quite hitting the centre of the target disc can be a displacement of the target nucleus from its original central position (see Lynds & Toomre 1976).

The 'spokes' of the Cartwheel, or the residual inner spiral arms, pose some interesting problems. As the intruding galaxy moves away from the disk, the decreasing excess radial gravitational force causes the orbits in the disk to relax rather violently causing the severe radial bunching discussed by Lynds & Toomre. Those orbits which were originally approximately circular become highly eccentric as a result of the interaction. The apogalacticon of those orbits which originally had a small radius can be inside the present radius of the ring. In other words some of the stars, if not the gas, will have started falling back towards the nucleus and any original clumpiness could show up, after the effects of differential rotation, as the spiral 'spokes'. The circular orbital period at the present radius of the ring is about 7×10^8 yr so that we would not yet expect such structure to be completely smeared out.

The small inner ring which is clearly visible in Plate 1 is an intriguing structure which may be connected with the different form of relaxation followed by those orbits which feel the interaction over a timescale which is long compared with an orbital period. Since the two nuclei are clearly not point masses, they themselves will feel a softened change in the gravitational potential as they pass through one another. Plate 1 also shows some evidence that galaxy 3 possesses a small ring with a size very similar to that of the small nuclear ring of the Cartwheel itself.

The luminosities derived for the individual H II regions are spectacularly high (Table 2) even when compared with the giant complexes in M101. It was noted above that these luminosities were not corrected for an A_V of $2^m.1$ which corresponds to $E_{B-V} = 0.64$ deduced from the Balmer decrement. A way of checking that the reddening was really internal would be to observe the radio free–free continuum and compare this with the measured H_β flux. Using the integrated H_β flux from the ring, uncorrected for extinction, the optically thin radio free–free continuum would be only about 0.2 mJy. This flux, however, could be significantly greater if there is a large amount of dust associated with the H II regions.

From the integrated H_β luminosity we can, however, estimate the number of stars which are responsible for ionizing the gas. Taking as typical an O6 main sequence star with an effective temperature of 40 000 K, the Lyman continuum luminosity is approximately

$$\int_{\nu_0}^{\infty} \frac{L\nu}{h\nu}\, d\nu \simeq 5 \times 10^{48} \text{ photons s}^{-1}$$

The total number of ionizing O6 stars is then

$$N(\mathrm{O6}) = \frac{L(\mathrm{H}_\beta)}{h\nu_{\mathrm{H}_\beta}} \frac{\alpha_{\mathrm{tot}}}{\alpha^{\mathrm{eff}}_{\mathrm{H}_\beta}} \cdot \frac{1}{5 \times 10^{48}}$$
$$\simeq 3 \times 10^5$$

where α_{tot} is the recombination coefficient to all levels.

The optical continuum energy distribution of knot A (knots B and C are very similar) is shown in Fig. 5, which suggests that most of the optical luminosity is coming from OB stars with a relatively small amount of reddening. Taking the absolute magnitude of a typical OB star to be $M_B = -5$, then the number of stars responsible for the integrated optical luminosity of the ring is about 3×10^6. The fact that this is an order of magnitude greater than the number estimated from the H_β flux probably just reflects the fact that it is only the very hottest stars which produce most of the Lyman continuum photons while all the stars contribute significantly to the optical continuum.

The high concentration of massive stars in the ring raises the question of the expected frequency of supernova outbursts. With the O-stars having a lifetime of only a few million years, the type II supernova rate could be as high as one per year. If each supernova has a total energy output of 10^{50} erg then such events would provide an energy input to the gas of approximately 3×10^{42} erg s^{-1}, which is large but still significantly smaller than the total observed optical emission line luminosity. This estimated supernova rate is therefore consistent with the observation that the gas is not collisionally ionized.

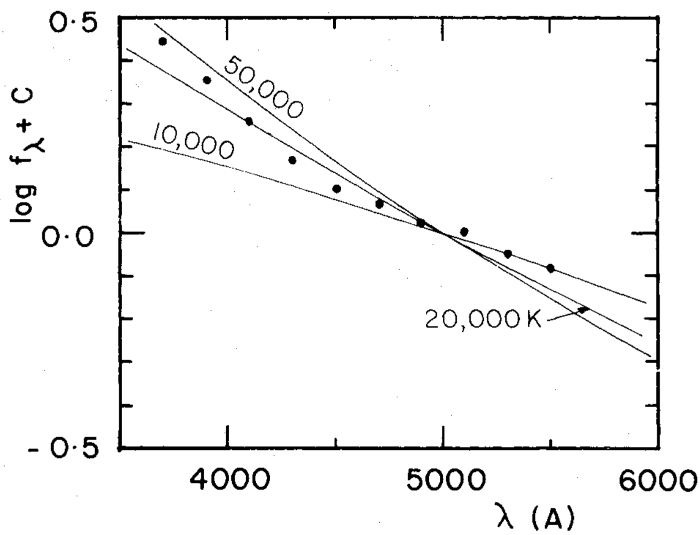

Figure 5. The optical continuum energy distribution of knot A (dots). The solid lines are unreddened black-body lines at the indicated temperatures, normalized to 5000 Å.

It is difficult to make a reliable estimate of the total mass of stars and gas in the ring itself, but if we take the mass-to-light ratio of extreme population I to be around one in solar units, then the mass comes out to be on the order of $2 \times 10^{10} M_\odot$. This is 5 per cent of the nuclear mass which was derived from the rotation of the ring. Using this mass and the observed velocity of expansion, the kinetic energy associated with the ring expansion is 2×10^{57} erg.

The Lynds & Toomre model is collisionless and therefore does not explicitly treat the behaviour of the gas content of the disk during the encounter. It seems reasonable, however, to suppose that the gas does get swept up as the ring moves outwards. Because A0035 now has such large dimensions, the ring may now contain the major fraction of the gas content of the whole galaxy. What is more, the gas should be well mixed by the inevitable shear within the ring, and thus the emission lines we observe should be representative of the mean composition of the gas content of the whole galaxy. Since the nitrogen and oxygen abundances are about an order of magnitude lower than in local H II regions like the Orion nebula in our Galaxy, a large fraction of the original gas content of A0035 was unprocessed through stars or supernova outbursts. This is either because the whole A0035 system is young or, as seems more likely, it had a massive halo of primordial gas which we are now privileged to see as a result of this improbable encounter. It is known from 21-cm line studies (Balkowski 1973; Dean & Davies 1975; Huchtmeier 1975; Rots 1975) that many galaxies of a type later than S0 contain quite massive neutral hydrogen clouds which extend outside the optical image. This can have a mass as large as $10^{10} M_\odot$ in some giant spirals like M101. If A0035 was originally similar to M101 then the present abundances tell us that the bulk of this halo consisted of primordial material and that the mass of the processed gas (if its abundances were on the average similar to Orion) was smaller by at least an order of magnitude.

Conclusions

We have seen that the particular type of galaxy–galaxy interaction proposed by Lynds & Toomre (1976) provides a consistent explanation of the morphology and the velocity structure of A0035. The sweeping up of interstellar gas by the expanding ring has led to rapid star formation and consequently to large numbers of OB stars and very luminous H II regions.

The rate of supernova explosions expected from such an extreme population I system may be as high as one per year. At the distance of A0035 a type II supernova at maximum light would have an apparent visual magnitude of 18 or 19, making a supernova search a relatively easy observational project with quite a good chance of success.

Acknowledgments

We are very grateful to Miller Goss, Ulrich Mebold and Hugo van Woerden for stimulating discussion and for observing A0035 in the 21-cm line at Parkes. We also thank Agris Kalnajs, John Danziger, John Whelan and Michael Penston for discussions, and Ann Savage, Andrew Wilson, David Malin, Ian Browne, John Straede and the AAT night assistants for assistance at the telescope and during some of the reductions. The Panel for the Allocation of Telescope Time generously provided clear nights for these observations. RAEF acknowledges support in the form of an SRC–AAT fellowship.

References

Arp, H. C. & Madore, B. F., 1975. *A catalogue of southern peculiar galaxies from the UK Schmidt survey: preliminary reduction of 36 fields,* Royal Observatory, Edinburgh.
Balkowski, C., 1973. *Astr. Astrophys.,* **29,** 43.
Cannon, R. D., Lloyd, C. & Penston, M. V., 1970. *Observatory,* **90,** 153.
Dean, J. F. & Davies, R. D., 1975. *Mon. Not. R. astr. Soc.,* **170,** 503.
de Vaucouleurs, G. & de Vaucouleurs, A., 1964. *Reference catalogue of bright galaxies,* The University of Texas Press, Austin.
Dufour, R. J., 1975. *Astrophys. J.,* **195,** 315.
Freeman, K. C. & de Vaucouleurs, G., 1974. *Astrophys. J.,* **194,** 569.
Graham, J. A., 1974. *Observatory,* **94,** 290.
Huchtmeier, W. K., 1975. *Astr. Astrophys.,* **45,** 259.
Lü, P. K., 1971. *Astr. J.,* **76,** 775.
Lynds, R. & Toomre, A., 1976. *Astrophys. J.,* **209,** 382.
Oke, J. B., 1974. *Astrophys. J. Suppl. Ser. 236,* **27,** 21.
Osterbrock, D. E., 1974. In *Astrophysics of gaseous nebulae,* W. H. Freeman and Co., San Francisco.
Peimbert, M. & Torres-Peimbert, Silvia, 1974. *Astrophys. J.,* **193,** 327.
Robinson, L. B. & Wampler, E. J., 1972. *Publ. astr. Soc. Pacific,* **84,** 161.
Robinson, L. B. & Wampler, E. J., 1973. *Astronomical observations with television type sensors,* p. 69, eds J. W. Glaspey & G. A. H. Walker, Vancouver, University of British Columbia.
Rots, A. H., 1975. *Astr. Astrophys.,* **45,** 43.
Seaton, M. J., 1975. *Mon. Not. R. astr. Soc.,* **170,** 475.
Saraph, H. E. & Seaton, M. J., 1970. *Mon. Not. R. astr. Soc.,* **148,** 367.
Theys, J. C., 1973. *PhD thesis,* Columbia University.
Vorontsov-Vel'yaminov, B. A. & Arkhipova, V. P., 1974. *The morphological catalogue of galaxies,* Moscow University.
Zwicky, F., 1941. *Applied mechanics,* Th. v. Kármán Anniversary volume, p. 137.